Available online at www.sciencedirect.com
ScienceDirect
Journal of Solid State Chemistry 180 (2007) 2616–2624
JOURNAL OF SOLID STATE CHEMISTRY
www.elsevier.com/locate/jssc

Preparation, spectroscopic properties of 1,4-di (*N*,*N*-diisopropylacetamido)-2,3(1*H*,4*H*)-quinoxalinedione (L) lanthanide complexes and the supramolecular structure of $[Nd_2L_2(NO_3)_6(H_2O)_2]\cdot H_2O$

Xue-Qin Song[a,b], Yang Yu[a], Wei-Sheng Liu[a,*], Wei Dou[a], Jiang-Rong Zheng[a], Jun-Na Yao[a]

[a]*College of Chemistry and Chemical Engineering, State Key Laboratory of Applied Organic Chemistry, Lanzhou University, Lanzhou 730000, China*
[b]*School of Chemical and Biological Engineering, Lanzhou Jiaotong University, Lanzhou 730070, China*

Received 11 April 2007; received in revised form 15 June 2007; accepted 20 June 2007
Available online 20 July 2007

Abstract

The reaction of lanthanide nitrate with 1,4-di (*N*,*N*-diisopropylacetamido)-2,3(1*H*,4*H*)-quinoxalinedione (L) yields six novel Ln(III) complexes ($[Ln_2L_2(NO_3)_6(H_2O)_2]\cdot H_2O$) which are characterized by elemental analysis, thermogravimetric analysis (TGA), conductivity measurements, IR, electronic and ^1H NMR spectroscopies. A new quinoxalinedione-based ligand is used as antenna ligand to sensitize the emission of lanthanide cations. The lowest triplet state energy level of the ligand in the nitrate complex matches better to the resonance level of Eu(III) and Sm(III) than Tb(III) and Dy(III) ion. The *f*–*f* fluorescence is induced in the Eu^{3+} and Sm^{3+} complexes by exciting into the π–π^* absorptions of the ligand in the UV. Furthermore, the crystal structures of a novel binuclear complex $[Nd_2L_2(NO_3)_6(H_2O)_2]\cdot H_2O$ has been determined by single-crystal X-ray diffraction. The binuclear $[Nd_2L_2(NO_3)_6(H_2O)_2]\cdot H_2O$ complex units are linked by the intermolecular hydrogen bonds and π–π interactions to form a two-dimensional (2-D) layer supramolecule.

Keywords: 2,3(1*H*,4*H*)-quinoxalinedione; Lanthanide complex; Crystal structure; Hydrogen bond; π–π interaction; Luminescence properties

1. Introduction

Although the 4*f* block ions display mainly the same formal charge (3+) and similar chemical properties, their coordination chemistry has become of increasing significance in the last few years. This is due to their electronic, magnetic and spectroscopic properties, which are different along the complete series and may be widely applied in various fields [1]. The favorable luminescence properties of lanthanides have fostered their application in the development of chemosensors [2–5], supramolecular devices such as logic gates [6,7], bioassays (e.g., for enzyme activity or DNA hybridization) [8], electroluminescent devices [9] or in optical telecommunication [10]. However, the application of lanthanide-based luminescence suffers from two serious drawbacks: (1) the poor light absorption properties and (2) the efficient non-radiative deactivation of their excited states by OH oscillators such as water [11]. In order to avoid these obvious disadvantages for the application of lanthanides, a strategy has been developed that involves the so-called antenna effect (Scheme 1). In this approach, the lanthanide ion is linked via complexation with a ligand, which includes an organic chromophore capable of absorbing light energy with a higher efficiency than the metal itself. In a subsequent energy transfer process, this chromophore acts as a sensitizer of the lanthanide-excited state, which can subsequently deactivate through luminescence. Owing to the large spectral gap between antenna excitation (often UV light) and emitted photons (visible to near IR), lanthanide-antenna conjugates have been often referred to as ''molecular devices for wavelength conversion'' [12]. Furthermore, complexation with a ligand provides lanthanides with a certain degree of protection

*Corresponding author. Fax: +86 931 8912582.
E-mail address: liuws@lzu.edu.cn (W.-S. Liu).

0022-4596/$ - see front matter © 2007 Elsevier Inc. All rights reserved.
doi:10.1016/j.jssc.2007.06.034

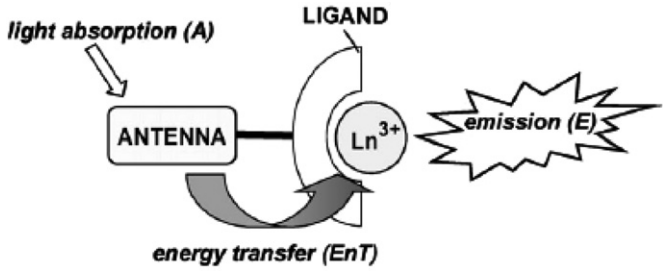

Scheme 1. Sensitization of lanthanide excited states by energy transfer from an antenna.

from surrounding water, hence, increasing their luminescence quantum yields.

Our group has been concentrating on the investigation of the supramolecular coordination chemistry and the luminescent properties of lanthanide (III) ions with the amide-type ligands which possess spheroidal cavities and hard binding sites. 2,3(1*H*,4*H*)-quinoxalinedione derivatives have been reported as excitatory amino acid antagonist with combined glycine/NMDA and AMPA receptor affinity [13–15]. However, their related coordination complexes as well as fluorescence properties have rarely been studied due to their low solubility [16]. In order to enhance the solubility as well as coordination ability of 2,3(1*H*,4*H*)-quinoxalinedione, we introduced a long amide chain to it and as continuation of our work on lanthanide coordination, we report here the synthesis, crystal structure and spectroscopic properties of the 1,4-di(*N*,*N*-diisopropylacetamido)-2,3(1*H*,4*H*)-quinoxalinedione (L) lanthanide complexes. To our best knowledge, they are the first examples of coordination structure of lanthanide complexes with 2,3(1*H*,4*H*)-quinoxalinedione ligand. Under excitation, Eu and Sm complex exhibited characteristic emissions. The lowest triplet state energy level of the ligand which was calculated from the phosphorescence spectrum of the Gd complex at 77 K indicates that the triplet state energy level of the ligand matches better to the resonance level of Eu(III) and Sm(III) than Tb(III) and Dy(III) ion.

2. Experimental

2.1. Materials

2,3-Dihydroxyquinoxaline was obtained from Aldrich Chemical Co. DMF was dried using 4 Å molecule sieves. The other commercially available chemicals were of A.R. grade and were used without further purification.

2.2. Methods

The metal ions were determined by EDTA titration using xylenol orange as an indicator. Combustion analyses were determined using a Vario EL elemental analyzer. The IR spectra were recorded on a Nicolet FT-170SX instrument using KBr disks in the 400–4000 cm^{-1}. Conductivity measurements were carried out with a DDS-307-type conductivity bridge using 1.0×10^{-3} mol dm^{-3} solutions in acetone at 25 °C. ^{1}H NMR spectra were measured on a Varian Mercury plus 400 spectrometer in $CDCl_3$ solution with TMS as internal standard. Thermogravimetric analyses (TGA) were performed with a WCT-2A thermoanalyzer under air atmosphere (30–700 °C) at a heating rate of 10 °C min^{-1}. Electronic spectra from 200 to 450 nm were recorded at room temperature using a Varian Cary 100 spectrophotometer. Fluorescence measurements were made on a Hitachi F-4500 spectrfluorophotometer equipped with quartz curettes of 1 cm path length. The samples of the solid-state fluorescence measurements are prepared as a powder film and the excitation and emission slit widths were 2.5 nm (in solid) and 5 nm (in solution), respectively.

2.3. Crystal structure determination

Suitable single crystal of the neodymium nitrate complex was carefully selected under an optical microscope and mounted in a fine-focus sealed tube. Crystallographic data for the compound was collected with graphite-monochromatic Mo$K\alpha$ radiation on a Bruker APEX area-detector diffractometer by the phi and omega scans technique. Primary non-hydrogen atoms were solved by direct method and refined anisotropically by full-matrix least-squares methods on F^2. The hydrogen atoms except for those of water molecules were generated geometrically. All calculations were performed using the programs SHELXS-97 and SHELXL-97. The $[Nd_2L_2(NO_3)_6(H_2O)_2]\cdot H_2O$ complex with chemical formula of $C_{48}H_{78}N_{14}Nd_2O_{29}$ crystallizes in the triclinic space group $P-1$, with lattice parameters $a=10.452(6)$ Å, $b=13.129(8)$ Å, $c=13.474(8)$ Å, $\alpha=93.603(7)^\circ$, $\beta=97.059(7)^\circ$, $\gamma=91.238(7)^\circ$, GOF = 1.066, $R1=0.0461$, w$R2=0.1115$, $Z=1$.

2.4. Synthesis of the ligand

α-Chloride-*N*,*N*-diisopropylacetamide was prepared according to the literature [17]. The ligand L (Scheme 2) was prepared according to the literature [18]. This ligand bears an amide chain to provide a diffluent ligand to complex lanthanide ions. ^{1}H NMR ($CDCl_3$, ppm): δ 7.19–7.16 (dd, 2H; quinoxaline: 5H and 8H); 6.99–6.96(dd, 2H; quinoxaline: 6H and 7H); 5.00(s, 4H, N–CH_2–C(O)); 4.09–4.05(m, 2H; N–CH–$(CH_3)_2$); 3.55–3.50(t, 2H; N–CH–$(CH_3)_2$); 1.37–1.13(t, 24H; $-CH_3$). Analytical data, Calc. for **L** (%): C, 64.84; H, 8.16; N, 12.60; Found (%): C, 64.97, H, 8.44, N, 12.23.

2.5. Syntheses of the complexes

To a stirred acetonitrile solution (5.0 mL) containing 0.1 mmol **L** was added 0.1 mmol $Ln(NO_3)_3\cdot 6H_2O$. The mixture was stirred for 8 h at room temperature. After removing solvents in vacuum, 10 mL ethyl acetate was added, the pale white precipitate was obtained and dried in vacuum over P_2O_5 for 48 h. All the complexes were

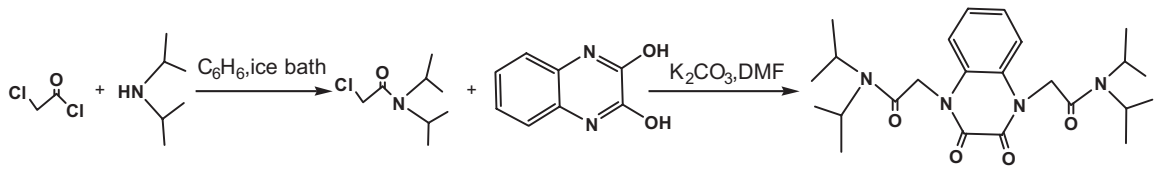

Scheme 2. The synthetic route of the ligand.

Table 1
Analytical and molar conductance data for the complexes (calculated values in parentheses)

Complex	Analysis (%)				Λm ($\Omega^{-1}\,cm^2\,mol^{-1}$)
	C	H	N	Ln	
$[Nd_2L_2(NO_3)_6(H_2O)_2]\cdot H_2O$	36.22(35.95)	4.81(4.90)	12.44(12.23)	17.72(17.99)	28.7
$[Sm_2L_2(NO_3)_6(H_2O)_2]\cdot H_2O$	35.98(35.68)	4.64(4.87)	12.39(12.13)	18.47(18.61)	35.0
$[Eu_2L_2(NO_3)_6(H_2O)_2]\cdot H_2O$	35.92(35.61)	4.65(4.86)	12.35(12.11)	18.59(18.77)	34.0
$[Gd_2L_2(NO_3)_6(H_2O)_2]\cdot H_2O$	35.69(35.38)	4.62(4.82)	12.28(12.03)	19.12(19.30)	28.4
$[Tb_2L_2(NO_3)_6(H_2O)_2]\cdot H_2O$	35.50(35.30)	4.75(4.81)	12.18(12.01)	19.18(19.46)	36.5
$[Dy_2L_2(NO_3)_6(H_2O)_2]\cdot H_2O$	35.05(34.95)	4.75(4.77)	11.92(11.89)	20.20(20.28)	27.8

obtained as white powders. Yield: 60–75%. Single crystals of complex were grown from ethyl acetate and acetonitrile (V:V = 10:1) mixed solution with slow evaporation at room temperature. After ca. 3 weeks, transparent crystals, which are suitable for X-ray diffraction analysis, were formed.

3. Results and discussion

Analytical data for the complexes, presented in Table 1, conformed to $[Ln_2L_2(NO_3)_6(H_2O)_2]\cdot H_2O$. All complexes are soluble in DMF, THF, acetonitrile, acetone, ethyl acetate, methanol and ethanol, but sparingly soluble in water, hexane and ether. The molar conductances of the complexes in acetone (see Table 1) indicate that all nitrate complexes act as non-electrolytes [19].

3.1. Crystal structure of $[Nd_2L_2(NO_3)_6(H_2O)_2]\cdot H_2O$

The crystal structure data and refinement details for $[Nd_2L_2(NO_3)_6(H_2O)_2]\cdot H_2O$ are given in Table 2. Selected bond lengths and bond angles are listed in Table 3. The structural information of other complexes has been obtained from the PXRD patterns. On the basis of X-ray powder diffraction studies, these complexes contain the same structural information with $[NdL_2(NO_3)_6(H_2O)_2]\cdot H_2O$. The Nd(III) complex contains two independent cations, each lying about an inversion center. Each Nd(III) ion is deca-coordinated by two oxygen atoms of **L** and seven O-atoms of three bidentate nitrates and the remaining one for water molecules (Fig. 1a). The coordination polyhedron is a distorted bicapped square antiprism. (Fig. 1b) The average distance between the Nd(III) ion and the coordination oxygen atoms is 2.536 Å, where the Nd–O12 is the shortest, probably owing to the higher electron density on the oxygen atom of the nitrate. The nitrate anion has proved to be a very useful ligand for the construction of coordination complex. Its anionic charge means that it usually plays the role of both bridging ligand and counterion (i.e., O5, O6, O8, O9 and O11 coordinate with Nd1 as terminal ligands, while O12 serves as a bridging atom to link two Nd atoms to form a binuclear unit). The deca-coordinated Nd ions are doubly bridged together through μ_2-nitrate ions with Nd⋯Nd distances of about 4.156(2) Å. Upon closer examination of the structure, It is interesting to note that the nitrate anion

Table 2
Crystal data and structure refinement for complex

Empirical formula	$C_{48}H_{78}N_{14}Nd_2O_{29}$
Formula weight	1603.72
Temperature	298(2) K
Wavelength	0.71073 Å
Crystal system, space group	Triclinic, $P-1$
Unit cell dimensions	$a = 10.452(6)$ Å, $\alpha = 93.603(7)$
	$b = 13.129(8)$ Å, $\beta = 97.059(7)$
	$c = 13.474(8)$ Å, $\gamma = 91.238(7)$
Volume	1830.5(19) $Å^3$
Z, calculated density	1,1.455 Mg/m^3
Absorption coefficient	1.487 mm^{-1}
$F(000)$	816
Crystal size	$0.56 \times 0.50 \times 0.12\,mm^3$
Theta range for data collection	1.96–25.01°
Limiting indices	$-12 \leqslant h \leqslant 11$, $-14 \leqslant k \leqslant 15$, $-16 \leqslant l \leqslant 15$
Reflections collected/unique	9287/6276 [R(int) = 0.0370]
Completeness to $\theta = 25.01$	97.2%
Absorption correction	Semi-empirical from equivalents
Max. and min. transmission	0.8417 and 0.4898
Refinement method	Full-matrix least-squares on F^2
Data/restraints/parameters	6276/289/428
Goodness-of-fit on F^2	1.066
Final R indices [$I > 2$sigma(I)]	$R1 = 0.0461$, w$R2 = 0.1115$
R indices (all data)	$R1 = 0.0667$, w$R2 = 0.1316$
Largest diff. peak and hole	1.794 and $-0.865\,e^{-3}$

Table 3
Selected bond lengths (Å) and angles (deg) for $[Nd_2L_2(NO_3)_6(H_2O)_2]\cdot H_2O$ complex

Nd(1)–(12)#1	2.400(4)	Nd(1)–O(14)	2.475(4)	Nd(1)–O(11)	2.490(5)	Nd(1)–O(1)	2.520(4)
Nd(1)–O(2)	2.551(4)	Nd(1)–O(6)	2.559(5)	Nd(1)–O(8)	2.576(5)	Nd(1)–O(12)	2.578(4)
Nd(1)–O(9)	2.580(4)	Nd(1)–O(5)	2.635(5)				

O(12)#1Nd(1)–O(14)	148.10(14)	O(12)#1Nd(1)–O(11)	117.86(14)	O(14)–Nd(1)—O(11)	73.67(15)
O(12)#1Nd(1)–O(1)	76.00(14)	O(14)–Nd(1)–O(1)	75.00(14)	O(11)–Nd(1)–O(1)	131.18(14)
O(12)#1Nd(1)–O(2)	79.91(14)	O(14)–Nd(1)–O(2)	75.24(13)	O(11)–Nd(1)–O(2)	73.50(14)
O(1)–Nd(1)–O(2)	62.86(12)	O(12)#1Nd(1)–O(6)	73.92(17)	O(14)–Nd(1)–O(6)	116.07(17)
O(11)–Nd(1)–O(6)	142.98(17)	O(1)–Nd(1)–O(6)	84.82(16)	O(2)–Nd(1)–O(6)	142.53(15)
O(12)#1Nd(1)–O(8)	131.33(15)	O(14)–Nd(1)–O(8)	79.23(15)	O(11)–Nd(1)–O(8)	75.70(16)
O(1)–Nd(1)–O(8)	132.59(14)	O(2)–Nd(1)–O(8)	144.33(15)	O(6)–Nd(1)–O(8)	71.79(18)
O(12)#1Nd(1)–O(12)	66.83(16)	O(14)–Nd(1)–O(12)	119.39(14)	O(11)–Nd(1)–O(12)	51.21(13)
O(1)–Nd(1)–O(12)	121.62(12)	O(2)–Nd(1)–O(12)	67.43(12)	O(6)–Nd(1)–O(12)	122.81(16)
O(8)–Nd(1)–O(12)	105.65(14)	O(12)#1Nd(1)–O(9)	87.36(15)	O(14)–Nd(1)–O(9)	124.43(14)
O(11)–Nd(1)–O(9)	74.74(16)	O(1)–Nd(1)–O(9)	153.61(15)	O(2)–Nd(1)–O(9)	134.70(14)
O(6)–Nd(1)–O(9)	70.79(18)	O(8)–Nd(1)–O(9)	49.14(15)	O(12)–Nd(1)–O(9)	67.57(15)
O(12)#1Nd(1)–O(5)	111.44(18)	O(14)–Nd(1)–O(5)	67.26(18)	O(11)–Nd(1)–O(5)	130.42(17)
O(1)–Nd(1)–O(5)	65.33(14)	O(2)–Nd(1)–O(5)	121.74(15)	O(6)–Nd(1)–O(5)	49.31(19)
O(8)–Nd(1)–O(5)	68.18(16)	O(12)–Nd(1)–O(5)	170.67(15)	O(9)–Nd(1)–O(5)	103.43(17)

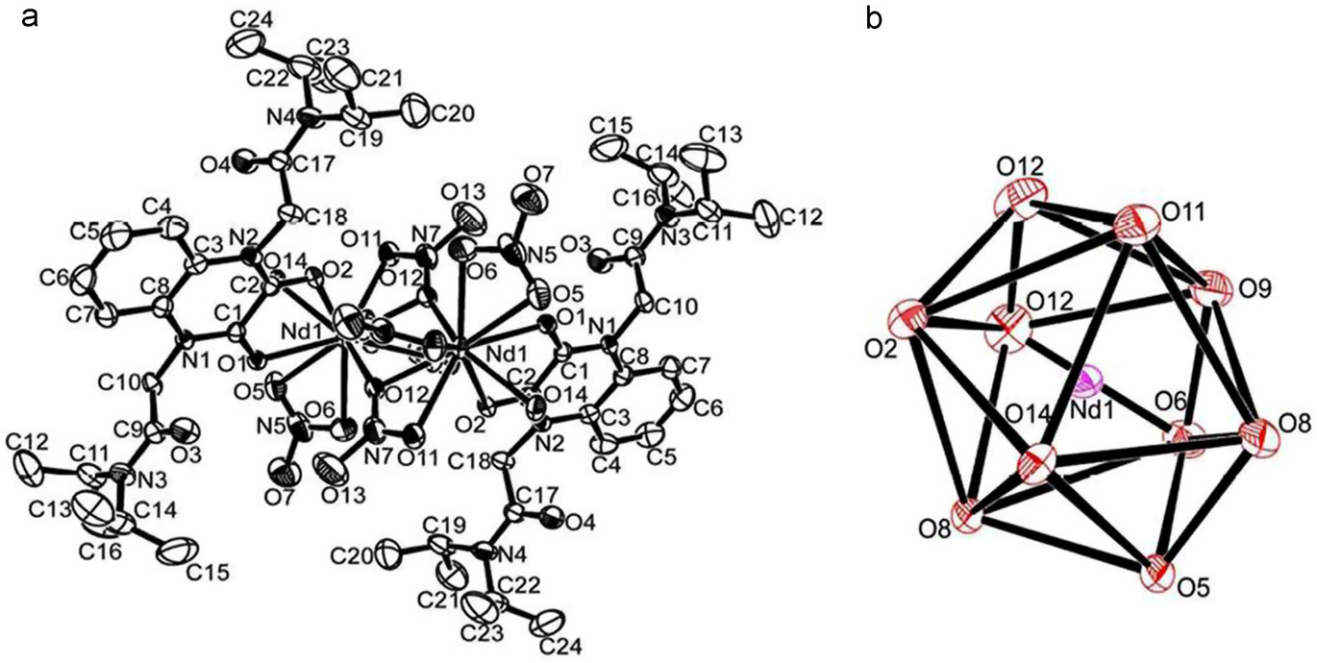

Fig. 1. (a) ORTEP diagram (30% probability ellipsoids) showing the coordination sphere of $[Nd_2L_2(NO_3)_6(H_2O)_2]\cdot H_2O$. (b) The coordination polyhedron of the Nd ion (30% probability ellipsoids).

functions not only as a chelate and a bridging ligand but also a hydrogen bond acceptor (O5) with a water molecule (O14) as a donor in the neighboring unit where the binuclear units are connected into one dimensional (1-D) chains via hydrogen bond with the D···A distance and D–H···A angle being 2.845(2) Å and 166.7(8)°, respectively (Fig. 2). In addition, the π–π stacking interactions between adjacent quinoxaline rings form a two-dimensional (2-D) layer supermolecule with the interplanar distance of 3.512 Å (Fig. 3).

3.2. Thermogravimetric analysis

The TGA diagrams performed under an air atmosphere show these complexes have similar stabilities and behaviors in the range of 35–700 °C, so we choose Nd(III) complex for detailed discussions (Fig. 4). The TGA study shows that Nd(III) complex losses weight from 239 °C, the gradual weight loss of 81.07% from 239 to 600 °C corresponds to the decomposition of the compound (calc. 79.04%) and the remaining weight of 18.93% is the Nd and O components

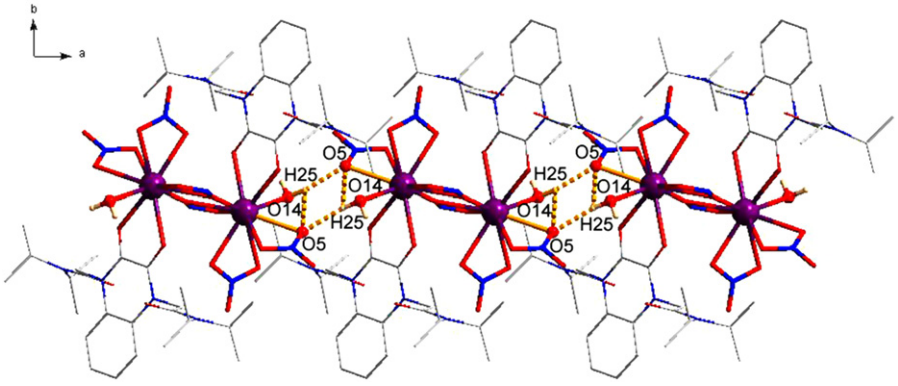

Fig. 2. The supramolecular chain generated by intermolecular hydrogen bonds of $[Nd_2L_2(NO_3)_6(H_2O)_2]\cdot H_2O$ (the hydrogen atoms except that of water molecular are omitted for clarity).

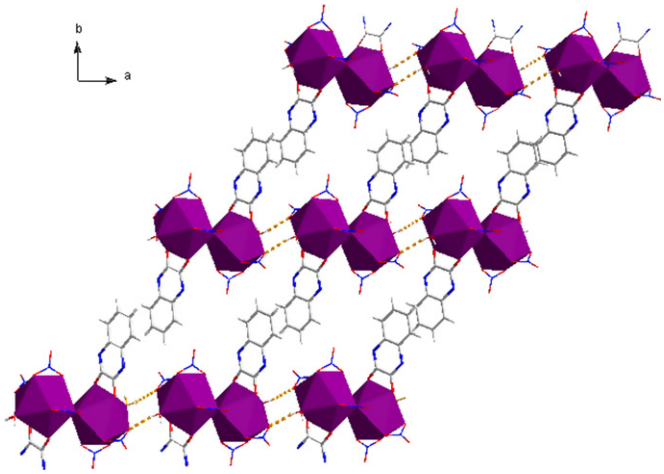

Fig. 3. 2-D supramolecular lay generated by intermolecular hydrogen bonds and π–π interactions of $[Nd_2L_2(NO_3)_6(H_2O)_2]\cdot H_2O$ (The terminal groups of the ligand and uncoordinated waters are omitted for clarity).

(calc. 20.96%). The X-ray powder diffraction pattern of the decomposition product obtained at 700 °C gave diffraction peaks corresponding to Nd_2O_3 and some other minor peaks belonging to unknown compounds.

3.3. IR spectra

The IR spectra of the lanthanide complexes are similar and the most important data is listed in Table 4. The infrared spectrum of the free ligand shows strong bands at about 1695 and 1646 cm^{-1}, the former is attributable to stretch vibration of the carbonyl group of 2,3(1*H*,4*H*)-quinoxalinedione (ν(C═O)), and the latter to carbonyl group of amide (ν(C═O)). In the IR spectra of the lanthanum complex, the peak of carbonyl of amide remains almost unchanged, but the peak of carbonyl of ketone red shifts by ca. 60 cm^{-1} as compared with the free ligand, thus indicating that only the oxygen atom of ketocarbonyl takes part in coordination to the lanthanide ion. The absorption bands assigned to the coordinated nitrate groups ($C2v$) are observed at about 1468 cm^{-1} (ν1), 1300 cm^{-1} (ν4), 1030 cm^{-1} (ν2) and 818 cm^{-1} (ν3) [20]. In addition, the separation of two strongest frequency bands $|\nu_1-\nu_4|$ lies in 162–170 cm^{-1}, clearly establishing that the NO_3^- groups in the solid complexes coordinate to the lanthanide ion as bidentate ligands [21]. And no band at 1380, 820 and 720 cm^{-1} in the spectra of complexes indicates that free nitrate groups (D_{3h}) are absent. Furthermore, broad bands at 3432 cm^{-1} could be attributed to the OH stretching vibrations of H_2O molecules.

3.4. Electronic spectra

The spectral profiles of the nitrate lanthanide complexes are also very similar. Absorption spectra of **L** and $[Eu_2L_2(NO_3)_3(H_2O)_2]\cdot H_2O$ are presented in Fig. 5(a). The electronic spectrum of the free ligand **L** displays two strong absorption band at 242 and 316 nm attributed to π–π^* transitions centered on the quinoxalinedione group. Upon complexation with lanthanide ion, the band centered at 242 nm hypsochromic shifts to 215 nm with a concomitant decrease in absorbance at 316 nm, which may be attributable to conformational changes of the ligand induced by the metal. Weak absorption bands of Nd complex was also observed at $\lambda = 490$–550, 550–640, 650–700, 715–775, 775–845 and 845–925 nm, as shown in Fig. 5(b). These absorption bands are attributed to the Nd(III) *f*–*f* transitions of $^4I_{9/2}$ (ground state)$\rightarrow{}^4G_{7/2}+{}^2G_{9/2}$, $^4I_{9/2}\rightarrow{}^4G_{5/2}+{}^2G_{7/2}$, $^4I_{9/2}\rightarrow{}^4F_{9/2}$, and $^4I_{9/2}\rightarrow{}^4F_{7/2}+{}^4S_{3/2}$, $^4I_{9/2}\rightarrow{}^4F_{5/2}+{}^2H_{9/2}$ and $^4I_{9/2}\rightarrow{}^4F_{3/2}$, respectively. According to Judd and Jorgensen [22], *f*–*f* transitions which obey $\Delta J = \pm 2$, $\Delta L = \pm 2$ selection rules are the most sensitive to the lanthanide ion environment, and are commonly referred to as hypersensitive. For Nd(III), the $^4I_{9/2}\rightarrow{}^4G_{5/2}$ absorption transition satisfies the above criteria, and, therefore, the intensity of this transition is often used as a probe of structural changes. In practice, the transition $^4I_{9/2}\rightarrow{}^2G_{7/2}$ is very close in energy, and particularly at room temperature, these two transitions must be analyzed together. The absorption transition $^4I_{9/2}\rightarrow{}^4F_{5/2}$ (~802.4 nm) also satisfies partially the selection rule for hypersensitive transitions and is used to monitor structural changes. This transition overlaps with the $^4I_{9/2}\rightarrow{}^2H_{9/2}$

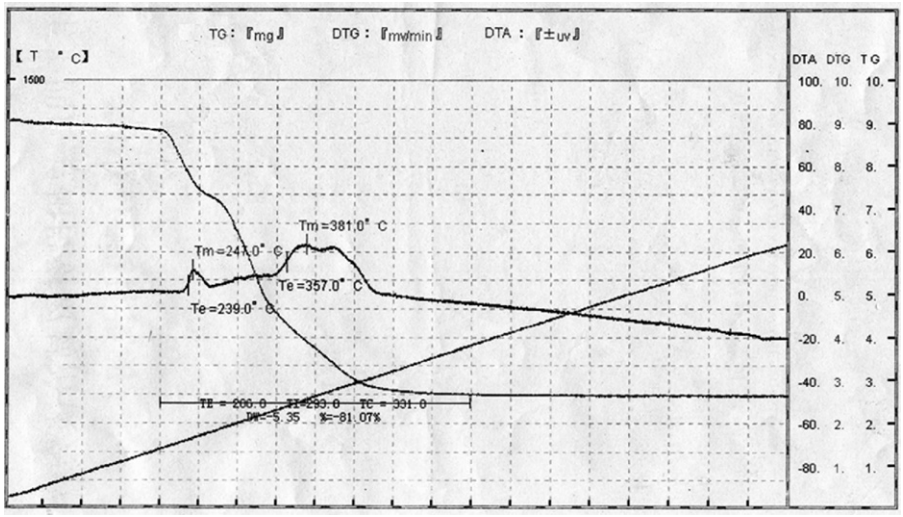

Fig. 4. TGA curve for Nd(III) complex.

Table 4
The most important IR bands (cm^{-1})

Compound	v (C=O)	v (C=O)	v_1 (NO_3^-)	v_4 (NO_3^-)	v_2 (NO_3^-)	v_3(NO_3^-)	$\lvert v_1-v_4\rvert$
L	1695	1646	–	–	–	–	–
$[Nd_2L_2(NO_3)_6(H_2O)_2]\cdot H_2O$	1635	1646	1469	1305	1037	818	164
$[SmL_2(NO_3)_6(H_2O)_2]\cdot H_2O$	1636	1644	1468	1298	1033	815	170
$[Eu_2(NO_3)_6(H_2O)_2]\cdot H_2O$	1637	1646	1469	1307	1037	819	162
$[Gd_2(NO_3)_6(H_2O)_2]\cdot H_2O$	1634	1645	1470	1308	1035	818	162
$[Tb_2(NO_3)_6(H_2O)_2]\cdot H_2O$	1636	1646	1468	1304	1036	818	164
$[Dy_2(NO_3)_6(H_2O)_2]\cdot H_2O$	1637	1643	1466	1287	1030	818	169

(~794 nm) transition. The electronic spectra in the visible region of the Nd(III) complex exhibits alterations in intensity and shifts in position of the absorption bands relative to the corresponding Ln(III) aquo ions. The shift has been attributed by Jørgensen to the effect of crystal fields upon interelectronic repulsion between the 4*f* electrons, and is related to covalence in the metal–ligand bond, assessed by Sinha's parameter (δ), the nephelauxetic ratio (β) [23,24]. The β value(1.0027) for Nd(III) complex is more than unity and δ value(−0.2718) is negative, suggesting that Nd^{3+}–O bond of the complex has weaker covalency than that of Nd^{3+} aquo ion.

3.5. Fluorescence studies

What interests us is the relationship between structure and properties. So the fluorescence characteristics of the solid complexes are detected. The luminescence of Ln^{3+} chelates is related to the efficiency of the intramolecular energy transfer between the triplet levels of the ligand and the emitting level of the ions, which depends on the energy gap between the two levels. In the intramolecular energy transfer, triplet state energy of the ligand is regarded as an important factor in excitation of the lanthanide ion [25,26]. In order to acquire the triplet excited state T_1 of the ligand **L**, the phosphorescence spectra of the Gd(III) nitrate complex was measured at 77 K in acetonitrile–methanol mixture (v:v, 1:10). The triplet state energy level T_1 of the ligand **L**, which was calculated from the shortest wavelength phosphorescence band of the corresponding Gd(III) complexes, is 18,910 cm^{-1} [27]. This energy level is above the lowest excited resonance level $^5D_0$(17,300 cm^{-1}) of Eu(III) and $^4G_{5/2}$(17,900 cm^{-1}) of Sm(III), but lower than the $^5D_4$(20,500 cm^{-1}) of Tb(III) and $^4F_{9/2}$(21,100 cm^{-1}) of Dy(III). Thus, the absorbed energy could be transferred from ligand to the Eu and Sm ions (Fig. 6) and the metal-centered emission is presented in Fig. 7. Actually, we do not observe the characteristic fluorescence of the Tb(III) and Dy(III) nitrate complex at room temperature which is entirely consistent with the observed efficient quenching of emission by the back-energy transfer process. It is well known that water molecules in the primary coordination sphere of Ln(III) have a strong deactivating effect, and the extent of this non-radiative deactivation pathway, which results in luminescence quenching, is inversely proportional to the energy gap between the excited state and the ground state manifold. The energy gap between $^5D_0$ and $^7F_6$ in Eu^{3+} matches the 2nd vibrational overtone of an O–H oscillator and the vibrational deactivation is therefore less efficient owing to a smaller Frank–Condon overlap between the two wavefunctions [28]. The intensity ratio of the $^5D_0$–$^7F_2$ transition to the $^5D_0$–$^7F_1$ transition is

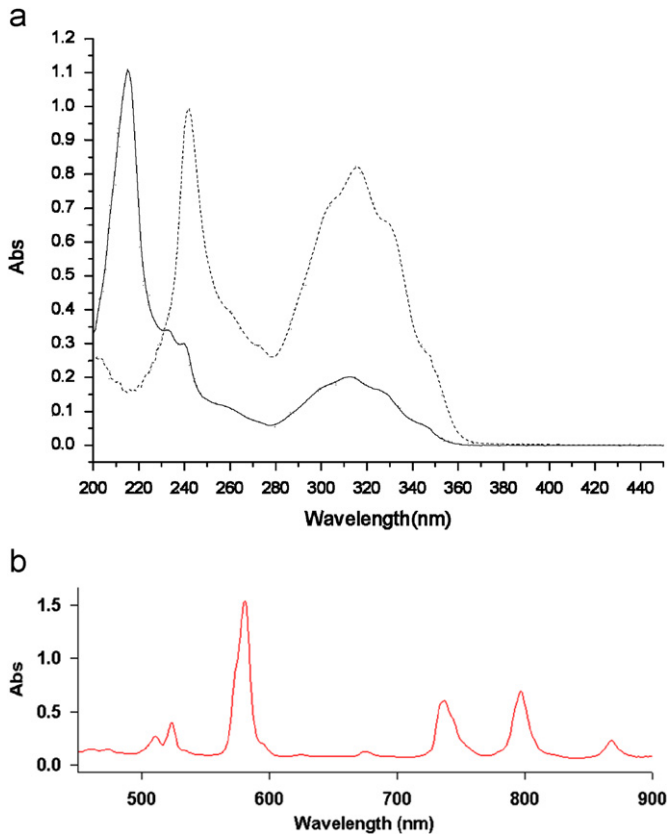

Fig. 5. (a) Absorption spectra of **L** (dotted line) and $[Eu_2L_2(NO_3)_3(H_2O)_2]\cdot H_2O$ (solid line)(1×10^{-5} M). (b) Absorption spectra of $[Nd_2L_2(NO_3)_3(H_2O)_2]\cdot H_2O$(0.02 M acetonitrile solution).

widely used as a measure of the coordination state and the site symmetry of the europium ion, since the $^5D_0$–$^7F_1$ emission is independent of the ligand environment, and primarily magnetic dipole in character, while the $^5D_0$–$^7F_2$ emission is essentially purely electric dipole in character, and its intensity is very sensitive to the crystal field symmetry. In the spectrum of Eu(III) complexes, the transition $^5D_0$–$^7F_2$ is the strongest in the four transitions with about four times the strength of the transition of $^5D_0$–$^7F_1$ (Table 5). The results show that Eu(III) has the lower symmetric coordination environment [29]. The fluorescence quantum yield **Φ** of the europium nitrate complex in acetonitrile (concentration: 1.0×10^{-5} mol L^{-1}) was found to be 0.43% with quinine sulfate as Ref. [30].

We can also see from Fig. 8 that in the four different solvents, the Eu(III) complex has the similar excitation and emission wavelengths, but the luminescence intensities for the europium complex become weaker from MeCN, ethyl acetate, acetone to THF solution (Table 5). This may be due to the coordinating effects of solvents, which is solvate effect [31]. Together with the raising coordination abilities of MeCN, ethyl acetate and acetone to THF for the lanthanide ions, the oscillatory motions of the entering molecules consume more energy, which the ligand triple level transfers to the emitting level of the lanthanide ion. Thus, the energy transfer could not be carried perfectly.

The suitability of the ligand as a sensitizer for Sm(III) luminescence was also examined (Table 5). Excitation of $[Sm_2L_2(NO_3)_6(H_2O)_2]\cdot H_2O$ in solid state at 367 nm leads

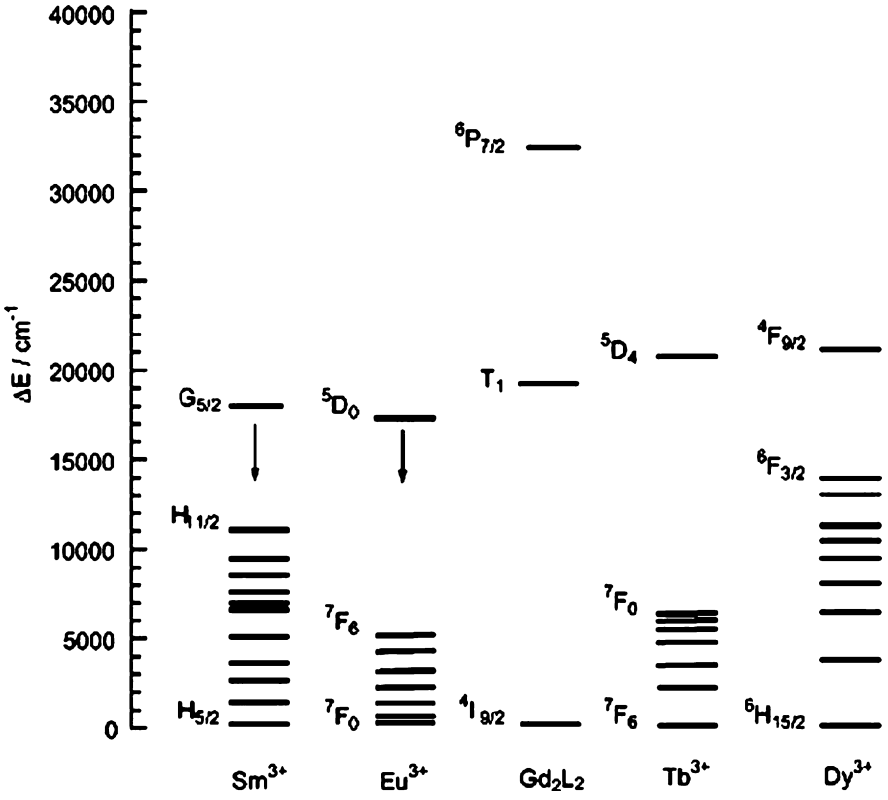

Fig. 6. Simplified energy diagram showing the lowest lanthanide excited state of the sensitizer **L** in the Gd(III) complex.

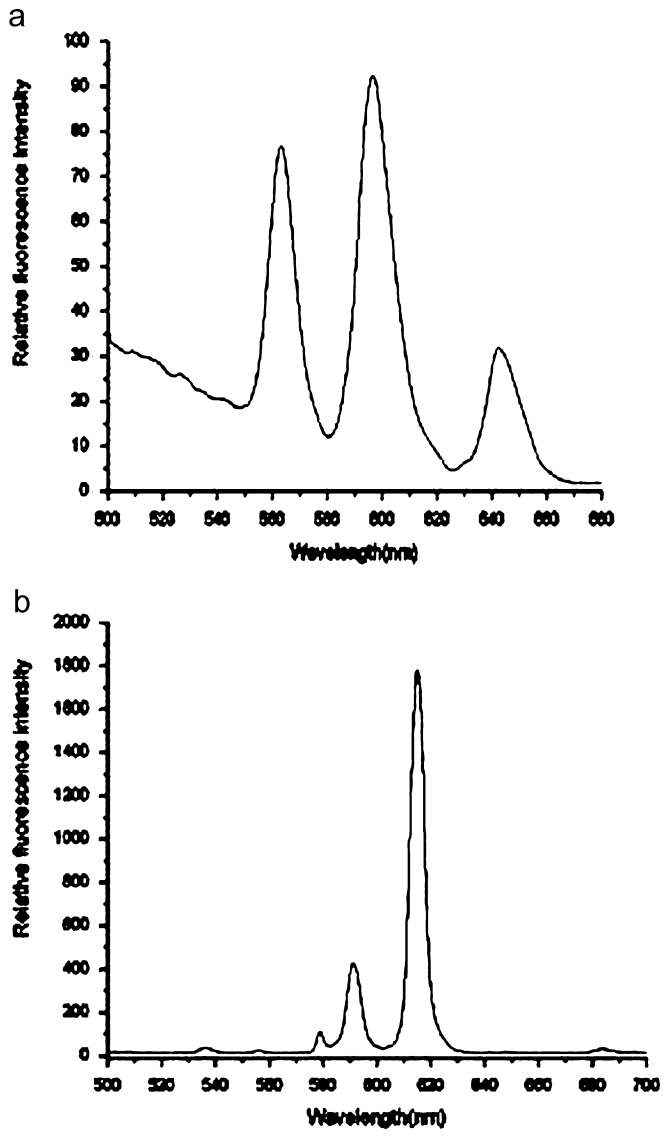

Fig. 7. (a) Emission spectrum of Sm(III) complex in solid state. (b) Emission spectrum of Eu(III) complex in solid state.

to moderate pink emission of Sm^{3+} due to $^4G_{5/2}$–^6H_J ($J = 5/2, 7/2, 9/2$) transitions (Fig. 7). The quantum yield of Sm was measured to be 0.12%. The value of quantum yield indicates that the ligand acts as a good sensitizer for Sm(III). Sm(III) complexes are known to have weak luminescence with the main source for non-radiative loss attributed to multiphonon emission [32]. Ligand to metal charge transfer transitions are higher in energy than those present in the relevant Eu(III) complexes, hence they do not lead to significant energy loss via radiationless quenching.

4. Conclusion

We have presented here the spectroscopic properties of lanthanide complexes with 2,3(1*H*,4*H*)-quinoxalinedione as well as the supramolecular structures of $[Nd_2L_2(NO_3)_6(H_2O)_2]\cdot H_2O$ which is the assemblies of the dinuclear

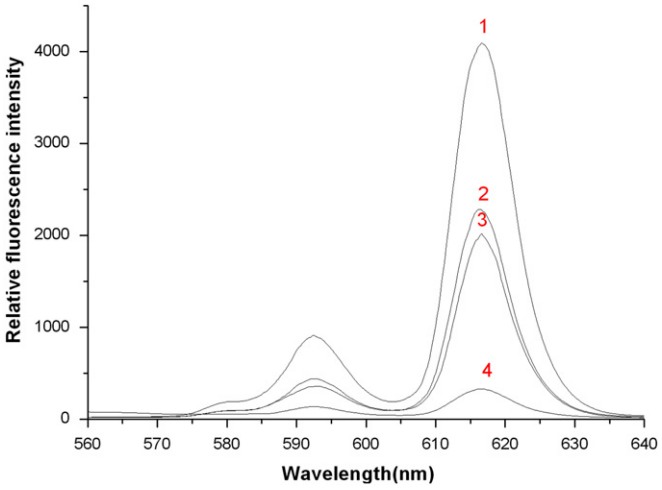

Fig. 8. Emission spectrum of $[Eu_2L_2(NO_3)_3(H_2O)_2]\cdot H_2O$ complex in different solutions at room temperature (concentration: 6×10^{-5} M). (1) In CH_3CN, (2) in ethyl acetate, (3) in acetone and (4) in THF.

Table 5
Fluorescence data for europium complex

Compound	Solvent	λ_{ex}(nm)	λ_{em}(nm)	RFI	Assignment
$[SmL_2(NO_3)_6(H_2O)_2]\cdot H_2O$	Solid state	367	563	76.73	$^4G_{5/2}\rightarrow{}^6H_{5/2}$
			597	92.49	$^4G_{5/2}\rightarrow{}^6H_{7/2}$
			642	31.90	$^4G_{5/2}\rightarrow{}^6H_{9/2}$
$[EuL_2(NO_3)_6(H_2O)_2]\cdot H_2O$	Solid state	370	579	113.4	$^5D_0\rightarrow{}^7F_0$
			591	422.5	$^5D_0\rightarrow{}^7F_1$
			615	1781	$^5D_0\rightarrow{}^7F_2$
			684	30.61	$^5D_0\rightarrow{}^7F_4$
	MeCN	365	592	913.2	$^5D_0\rightarrow{}^7F_1$
			616	4096	$^5D_0\rightarrow{}^7F_2$
	AcOEt	360	592	361.4	$^5D_0\rightarrow{}^7F_1$
			617	2283	$^5D_0\rightarrow{}^7F_2$
	Acetone	360	592	441.6	$^5D_0\rightarrow{}^7F_1$
			616	2020	$^5D_0\rightarrow{}^7F_2$
	THF	364	592	137.8	$^5D_0\rightarrow{}^7F_1$
			616	329.2	$^5D_0\rightarrow{}^7F_2$

complex units via the intermolecular hydrogen bonds and π–π stacking interactions. Excitation of π–π^* transitions of the ligand is followed by efficient energy transfer to *f*–*f* excited states in Eu (III) and Sm(III) complexes. In particular, the kinds of results presented here should help to design useful agents exploiting luminescence properties of lanthanide complexes rationally.

5. Supplementary material

Crystallographic data for the structural analysis have been deposited with the Cambridge Crystallographic Data Center, CCDC No. 627773. Copies of this information may be obtained free of charge from the director, CCDC, 12 Union Road, Cambridge CB2 IEZ, UK (e-mail: deposit@ccdc.cam.ac.uk or www: http://www.ccdc.cam.ac.uk).

Acknowledgments

This work was supported by the National Natural Science Foundation of China (Grants 20431010, 20621091 and J 0630962).

References

[1] R.S. Puche, P. Caro (Eds.), Rare Earths, Editorial Complutense, Madrid, 1998.
[2] A.P. de Silva, H.Q. Nimal Gunaratne, T.E. Rice, S. Stewart, Chem. Commun. (1997) 1891.
[3] D. Parker, P.K. Senanayake, J.A.G. Williams, J. Chem. Soc.—Perkin Trans. 2 (1998) 2129.
[4] L.J. Charbonniere, R. Ziessel, M. Montalti, L. Prodi, N. Zaccheroni, C. Boehme, G. Wipff, J. Am. Chem. Soc. 124 (2002) 7779.
[5] W.S. Liu, T.Q. Jiao, Y.Z. Li, Q.Z. Liu, M.Y. Tan, H. Wang, L.F. Wang, J. Am. Chem. Soc. 126 (2004) 2280.
[6] T. Gunnlaugsson, D.A. Mac Doó naill, D. Parker, J. Am. Chem. Soc. 123 (2001) 12866.
[7] M. de Sousa, M. Kluciar, S. Abad, M.A. Miranda, B. de Castroand, U. Pischel, Photochem. Photobiol. Sci. 3 (2004) 639.
[8] H. Bazin, M. Pré audat, E. Trinquet, G. Mathis, Spectrochim. Acta Part A 57 (2001) 2197.
[9] J. Kido, Y. Okamoto, Chem. Rev. 102 (2002) 2357.
[10] K. Kuriki, Y. Koike, Y. Okamoto, Chem. Rev. 102 (2002) 2347.
[11] S.W. Magennis, S. Parsons, Z. Pikramenou, Chem.—Eur. J. 8 (2002) 5761.
[12] J.-M. Lehn, Supramolecular Chemistry—Concepts and Perspectives, first ed., VCH, Weinheim, 1995.
[13] M.J. Fray, D.J. Bull, C.L. Carr, E.C.L. Gautier, C.E. Mowbray, A. Stobie, J. Med. Chem. 44 (2001) 1951.
[14] G.P. Sun, N.J. Uretsky, L.J. Wallace, G. Shams, D.M. Weinstein, D.D. Miller, J. Med. Chem. 39 (1996) 4430.
[15] H.W. Yoo, M.E. Suh, S.W. Park, J. Med. Chem. 41 (1998) 4716.
[16] A. Fujimoto, A. Sakurai, E. Iwase, Bull. Chem. Soc. Japan 49 (1976) 809.
[17] H. Röhnert, Arch. Pharm. 293 (1960) 573.
[18] Y.-L. Zhang, W.-S. Liu, W. Dou, W.-W Qin, Spectrochim. Part A 60 (2004) 1707.
[19] W.J. Gear, Coor. Chem. Rev. 7 (1971) 81.
[20] K. Nakamoto, Infrared and Raman spectra of Inorganic and Coordination Compounds, third ed., Wiley, New York, 1978, 227pp.
[21] N.F. Curtis, Y.M. Curtis, Inorg. Chem. 4 (1964) 804.
[22] C.K. Jorgensen, B.R. Judd, Mol. Phys. 8 (1964) 281.
[23] S.P. Sinha, Spectrochim. Acta 22 (1966) 57.
[24] M. Albin, R.R. Wright Jr., W.D. Horrochs, Inorg. Chem. 24 (1985) 2491.
[25] M.L. Bhaumic, M.A. El-Sayed, J. Phys. Chem. 69 (1965) 275.
[26] W. Dawson, J. Kropp, M. Windsor, J. Chem. Phys. 45 (1966) 2410.
[27] G.A. Crosby, R.E. Whan, R.M. Alire, J. Chem. Phys. 34 (1961) 743.
[28] W.D. Horrocks Jr., D.R. Sudnick, Acc. Chem. Res. 14 (1981) 384.
[29] W.S. Liu, M.Y. Tan, X. Wang, S.Y. Zhang, Acta Chim. Sin. 48 (1990) 1090.
[30] C.A. Parker, W.T. Rees, Analyst 85 (1960) 587;
W. Yang, Z.L. Mo, X.L. Teng, M. Chen, J.Z. Gao, L. Yuan, J.W. Kang, Q.Y. Ou, Analyst 123 (1998) 1745.
[31] H.Q. Liu, T.C. Cheung, C.M. Che, Chem. Commun. (1996) 1039.
[32] N. Sabbatini, S. Dellonte, G. Blasse, Chem. Phys. Lett. 129 (1986) 541.